

Article

Thermal, Optical, and IR-Emission Properties of Extremely Low Hydroxyl $\text{TeO}_2\text{-WO}_3\text{-Bi}_2\text{O}_3\text{-La}_2\text{O}_3\text{-xEr}_2\text{O}_3$ Glasses for Mid-Infrared Photonics

Vitaly V. Dorofeev ^{1,2}, Vasily V. Koltashev ³, Sergei E. Motorin ^{1,2} , Alexander D. Plekhovich ¹ and Arkady V. Kim ^{2,*}

- ¹ G.G. Devyatykh Institute of Chemistry of High-Purity Substances of the Russian Academy of Sciences, 49 Tropinin Str., 603951 Nizhny Novgorod, Russia; dorofeev@ihps-nnov.ru (V.V.D.); motorin@ihps-nnov.ru (S.E.M.); plekhovich@ihps-nnov.ru (A.D.P.)
- ² Institute of Applied Physics of the Russian Academy of Sciences, 46 Ulyanov Str., 603950 Nizhny Novgorod, Russia
- ³ Prokhorov General Physics Institute of the Russian Academy of Sciences, Dianov Fiber Optics Research Center, 38 Vavilov Str., 119333 Moscow, Russia; kvv@fo.gpi.ru
- * Correspondence: arkady.kim@gmail.com

Abstract: A series of glass samples of the tungsten–tellurite system $\text{TeO}_2\text{-WO}_3\text{-Bi}_2\text{O}_3\text{-(4-x)La}_2\text{O}_3\text{-xEr}_2\text{O}_3$, $x = 0; 0.4; 0.5; 0.7; 1.2; 2; 4$ mol%, $C_{\text{Er}} = 0 - 15 \times 10^{20} \text{ cm}^{-3}$ were synthesized from high-purity oxides in an oxygen flow inside a specialized sealed reactor. In all samples of the series, an extremely low content of hydroxyl groups was achieved ($\sim n \times 10^{16} \text{ cm}^{-3}$, more than 4 orders of magnitude lower than the concentration of erbium ions), which guarantees minimal effects on the luminescence properties of Er^{3+} . The glasses are resistant to crystallization up to 4 mol% Er_2O_3 , and the glass transition temperatures do not depend on the concentration of erbium oxide when introduced by replacing lanthanum oxide. Thin 0.2 mm plates have high transmittance at a level of 20% in the 4.7–5.3 μm range, and the absorption bands of hydroxyl groups at about 2.3, 3, and 4.4 μm , which are typical for ordinary tellurite glass samples, are indistinguishable. The introduction of erbium oxide led to an insignificant change in the refractive index. Er_2O_3 -concentration dependences of the luminescence intensities and lifetimes near the wavelengths of 1.53 and 2.75 μm were found for the $^4\text{I}_{13/2}\text{-}^4\text{I}_{15/2}$ and $^4\text{I}_{11/2}\text{-}^4\text{I}_{13/2}$ transitions of the Er^{3+} ion. The data obtained are necessary for the development of mid-infrared photonics; in particular, for the design of Er^{3+} -doped fiber lasers.

Keywords: high-purity tellurite glass; Er_2O_3 content; hydroxyl groups; crystallization; glass transition temperature; luminescence; lifetime



Citation: Dorofeev, V.V.; Koltashev, V.V.; Motorin, S.E.; Plekhovich, A.D.; Kim, A.V. Thermal, Optical, and IR-Emission Properties of Extremely Low Hydroxyl $\text{TeO}_2\text{-WO}_3\text{-Bi}_2\text{O}_3\text{-La}_2\text{O}_3\text{-xEr}_2\text{O}_3$ Glasses for Mid-Infrared Photonics. *Photonics* **2021**, *8*, 320. <https://doi.org/10.3390/photonics8080320>

Received: 12 July 2021

Accepted: 3 August 2021

Published: 9 August 2021

Publisher's Note: MDPI stays neutral with regard to jurisdictional claims in published maps and institutional affiliations.



Copyright: © 2021 by the authors. Licensee MDPI, Basel, Switzerland. This article is an open access article distributed under the terms and conditions of the Creative Commons Attribution (CC BY) license (<https://creativecommons.org/licenses/by/4.0/>).

1. Introduction

Modern-day applications of mid-infrared photonics, which encompasses the generation, manipulation, transmission, and detection of mid-IR radiation, have undoubtedly become possible with the technological advancements in the material growth and formation of new composites, particularly of specialty glasses, such as chalcogenide, fluoride, and telluride glasses, with their unique properties, relevant for use in photonic devices. Here, we will pay special attention to the tellurite glasses, due to their distinctive properties: they are transparent in a wide spectral range of 0.4–5.5 μm ; have good chemical stability and solubility of rare-earth oxides; the best compositions are sufficiently stable against crystallization; and low phonon energy makes it possible to achieve stimulated emission at electronic transitions of rare-earth ions, which are nonradiative for most oxide glasses [1–6]. This allows the use of glasses based on tellurium dioxide as active media for fiber-optic devices in the IR range of 1–3 μm , in which the most important area of application lies beyond 2.2 μm , where step-index silicate fibers are inoperative. Tellurite glass fibers are efficient up to 3–3.5 μm [7], are transparent in the pumping range up to 1 μm , and have

already demonstrated the ability for lasing in active fibers, including generation near 2.3 μm [8,9].

At present, fiber laser sources in the 1–3 μm range are in great demand for solving many fundamental and applied problems. Due to the presence of absorption bands of many inorganic and organic molecules, primarily absorption bands of hydroxyl groups in solids (including biological tissues) [9–13], such sources are in demand in laser surgery, cosmetic medicine, atmospheric monitoring systems, remote sensing, and diagnostics, as well as for the well-known needs of telecommunications and radiophotonics.

In this work, tungsten-tellurite glass containing lanthanum and bismuth oxides was chosen as a matrix composition for the introduction of erbium. Among most tellurite glass compositions, systems based on $\text{TeO}_2\text{-WO}_3$ have the advantages of higher glass transition temperatures, nonlinear optical properties, and crystallization resistance, and have a relatively low thermal expansion. Resistance to crystallization can be significantly improved by using high-purity starting materials [14] and modifying the glass composition with lanthanum oxide La_2O_3 . Some $\text{TeO}_2\text{-WO}_3\text{-La}_2\text{O}_3$ glasses are extremely resistant to crystallization in a wide range of La_2O_3 concentrations [2,15,16]. In addition, the presence of lanthanum oxide in the glass composition allows the introduction of active additives of other rare earth oxides instead of La_2O_3 , without significant changes in the physicochemical properties. The Bi_2O_3 additive is used to create fiber structures by modifying the refractive index of the core. Bismuth oxide is excellently soluble in tungsten–tellurite matrices, has a positive effect on the stability of some compositions to crystallization [6,16,17], and significantly increases the linear and nonlinear refractive indices [18,19].

Thus, $\text{TeO}_2\text{-WO}_3\text{-La}_2\text{O}_3\text{-Bi}_2\text{O}_3$ tellurite glass is a good candidate for the manufacture of step-index fibers [15,16].

Studies of the thermal, optical, and emission properties of erbium-doped tellurite glasses of various compositions have been of considerable interest to researchers for several decades. In [20], the effect of the addition of Er_2O_3 on the thermodynamic functions of the tungsten–tellurite system $\text{TeO}_2\text{-WO}_3\text{-La}_2\text{O}_3\text{-Bi}_2\text{O}_3$ was studied from the point of view of developing a method for predicting the thermodynamic properties of unexplored glass compositions.

G.N. Boetti et al. [21] fabricated samples as follows: $\text{TeO}_2\text{-WO}_3\text{-Na}_2\text{O-Nb}_2\text{O}_5\text{-xEr}_2\text{O}_3$, where $x = 0.01, 0.1, 0.5, 1, 3$ wt%. The glass transition temperature and glass density were found to increase monotonically with Er_2O_3 content. The refractive index of the glasses decreased with increasing Er^{3+} ion content. While pumped with a commercial telecom 980 nm laser diode, the 1.5 μm emission band became broader with the increasing concentration of Er ions. The maximum doping concentration allowed was found to be around 1.77×10^{20} ions/ cm^3 , for which a lifetime of 3.4 ms for the ${}^4\text{I}_{13/2}$ level was measured. The lifetime of the ${}^4\text{I}_{13/2}$ state decreased with increasing Er ion concentration, due to the energy transfer process. The longest lifetime of 3.7 ms was measured for the sample with a doping level of 8.9×10^{19} ions/ cm^3 . The lifetime of the ${}^4\text{I}_{11/2}$ state of Er^{3+} remained unchanged with the increase of its concentration and was at a level of 140 ± 30 μs . Quaternary tellurite glass systems $\text{TeO}_2\text{-WO}_3\text{-TiO}_2\text{-xEr}_2\text{O}_3$ with $x = 0.01, 0.1, 1, 3, 5,$ and 7 mol% of Er_2O_3 were prepared and investigated in [22]. All the samples possessed a thermal stability higher than 100 K, except the glass sample with 7 mol% of Er_2O_3 characterized by a low thermal stability of 74 K. The glass transition temperature significantly increased with the Er_2O_3 content, increasing from 0.01 to 7 mol% [22]. The authors of [23] studied the influence of Er_2O_3 addition on the thermal behavior of tungsten–tellurite glasses $\text{TeO}_2\text{-WO}_3$ doped with 0.5 and 1.0 mol% of Er_2O_3 by running detailed differential thermal analyses. Introducing rare-earth elements into tungsten–tellurite glasses and increasing their content resulted in an increase in glass transition temperatures.

The erbium ion in the tellurite matrix in the IR region is characterized by three luminescence bands, with maxima of $\sim 1, \sim 1.55,$ and ~ 2.75 μm , corresponding to the electronic transitions ${}^4\text{I}_{11/2}\text{-}{}^4\text{I}_{15/2}, {}^4\text{I}_{13/2}\text{-}{}^4\text{I}_{15/2},$ and ${}^4\text{I}_{11/2}\text{-}{}^4\text{I}_{13/2}$ [24]. However, for a long time, studies of the luminescence properties of the erbium ion focused on emission from

the long-lived ${}^4I_{13/2}$ level. This is due to the fast nonradiative relaxation of the ${}^4I_{11/2}$ level by hydroxyl groups in tellurite glasses obtained by a trivial method in air. Only with the advent of progressive methods for drying the melt, was the study of the emission of about 2.75 μm intensified.

The most convenient absorption band for the activation of the Er^{3+} ion in tellurite glasses is the absorption band at about 980 nm, which corresponds to the wavelengths of inexpensive standard commercial laser diodes. In this case, the level of ${}^4I_{11/2}$ is excited, and then the transition from the ${}^4I_{11/2}$ level to ${}^4I_{13/2}$ occurs. For silica glass, due to the high phonon energy, the level of ${}^4I_{11/2}$ is depopulated without radiation, but for tellurite glasses, a radiative transition in the 2.7–2.8 μm range is possible. The ${}^4I_{13/2}$ level is filled, and generation in the range of 1.53–1.6 μm can be achieved at the ${}^4I_{13/2}$ – ${}^4I_{15/2}$ transition [25,26].

The influence of the concentration of Er^{3+} ions on the luminescent properties of TeO_2 - WO_3 - ZnO glasses was studied in [27]. It was noted that with an increase in the concentration of Er^{3+} ions from 1.66×10^{20} to $4.11 \times 10^{20} \text{ cm}^{-3}$, the intensity and width of the luminescence band of about 1.5 μm increase, and the decay time of luminescence decreases from 3.6 ms to 3.3 ms, which indicates the appearance of concentration quenching.

Luminescence in the 2.7–2.8 μm region at the ${}^4I_{11/2}$ – ${}^4I_{13/2}$ transition in tellurite glasses was studied in [24,25,28]. For various compositions of tungsten–tellurite glasses, the lifetime of the ${}^4I_{11/2}$ level ($\sim 100 \mu\text{s}$) is much shorter than the lifetime of the ${}^4I_{13/2}$ level (several ms), due to the moderate phonon energy of $\sim 900 \text{ cm}^{-1}$ [2,5,25]. With continuous wave (CW) pumping at the ${}^4I_{15/2}$ – ${}^4I_{11/2}$ transition, this leads to a high population at the ${}^4I_{13/2}$ level and a small population at the ${}^4I_{11/2}$ level. Under laser pumping at 978 nm in Er^{3+} doped tungsten–tellurite glasses, the luminescence intensity in the 2.7 μm region increased with increasing concentration of Er_2O_3 [24].

The main channel of nonradiative relaxation in tellurite glasses activated with Er^{3+} is quenching on vibrations of OH groups. Due to the presence of an OH absorption band of about 3 μm , the internal energy of Er^{3+} at the ${}^4I_{13/2}$ level is converted into the vibration energy of two hydroxyl groups. As a result, OH ions cause both nonradiative relaxation of the excited energy level and absorption of Er^{3+} luminescence radiation at a wavelength of about 1.5 μm . These effects are even more pronounced at the ${}^4I_{11/2}$ – ${}^4I_{13/2}$ transition, since only one hydroxyl group is involved [29]. Thus, to obtain an active medium for lasing, it is especially important to synthesize and study only glass with a minimum hydroxyl concentration.

There has been a significant number of publications studying the properties of various erbium-activated tellurite glass compositions. However, information about the properties of erbium-activated glasses of the lanthanum–tungsten–tellurite system is insufficient, although they have already proven their promise for fiber optics applications [5,7,30].

In connection with the above, in this work we studied the properties of TeO_2 - WO_3 - Bi_2O_3 - La_2O_3 - $x\text{Er}_2\text{O}_3$ glasses, which are important for use in fiber optics, depending on the erbium concentration. Crystallization stability, glass transition temperatures, the transmission spectra and absorption bands of Er^{3+} and OH groups, refractive indices, and luminescence characteristics were studied. To obtain the most accurate data, special attention was paid to reducing the concentration of impurities, primarily hydroxyl groups, through the use of pure starting materials and original synthesis technology.

2. Materials and Methods

2.1. Glass Samples Preparation

Erbium-doped tungsten–tellurite glasses were produced by melting the oxides in crucibles of platinum inside a sealed silica chamber in an atmosphere of purified oxygen. A “TWBL- $x\text{Er}$ ” series of glass compositions with a common formula TeO_2 - WO_3 -(4- x) La_2O_3 - Bi_2O_3 - $x\text{Er}_2\text{O}_3$, where $x = 0; 0.4; 0.5; 0.7; 1.2; 2; 4 \text{ mol}\%$, was produced. The compositions of the glasses of the studied series, designations, the content of the erbium oxide dopant, and hydroxyl groups absorption at $\sim 3 \mu\text{m}$ are listed in Table 1.

Table 1. The compositions of glasses of the studied TWBL-xEr series, designations, the content of the erbium oxide dopant, and hydroxyl group absorption at $\sim 3 \mu\text{m}$.

Composition, mol%	Designation of the Glasses	Er ₂ O ₃ Content, mol%	Er ³⁺ Ions Content, cm ⁻³	OH Groups Volume Absorption at $\sim 3 \mu\text{m}$, cm ⁻¹
71.2TeO ₂ -23.7WO ₃ -1.1Bi ₂ O ₃ -4La ₂ O ₃ -0Er ₂ O ₃	TWBL-0Er	0	0	-
71.2TeO ₂ -23.7WO ₃ -1.1Bi ₂ O ₃ -3.6La ₂ O ₃ -0.4Er ₂ O ₃	TWBL-0.4Er	0.4	1.54×10^{20}	0.003
71.2TeO ₂ -23.7WO ₃ -1.1Bi ₂ O ₃ -3.5La ₂ O ₃ -0.5Er ₂ O ₃	TWBL-0.5Er	0.5	1.93×10^{20}	0.005
71.2TeO ₂ -23.7WO ₃ -1.1Bi ₂ O ₃ -3.3La ₂ O ₃ -0.7Er ₂ O ₃	TWBL-0.7Er	0.7	2.7×10^{20}	0.005
71.2TeO ₂ -23.7WO ₃ -1.1Bi ₂ O ₃ -2.8La ₂ O ₃ -1.2Er ₂ O ₃	TWBL-1.2Er	1.2	4.61×10^{20}	0.006
71.2TeO ₂ -23.7WO ₃ -1.1Bi ₂ O ₃ -3.5La ₂ O ₃ -2Er ₂ O ₃	TWBL-2Er	2	7.64×10^{20}	0.011
71.2TeO ₂ -23.7WO ₃ -1.1Bi ₂ O ₃ -0La ₂ O ₃ -4Er ₂ O ₃	TWBL-4Er	4	15.2×10^{20}	0.009

The gradation of the erbium oxide concentration was achieved by lanthanum oxide replacement. All the samples were synthesized with a low and approximately equal hydroxyl content, corresponding to OH-group volume absorption at the level of $n \times 10^{-3} \text{ cm}^{-1}$ at a wavelength of $\sim 3 \mu\text{m}$; the concentrations of Er³⁺ were in the range of 1.54×10^{20} – $15 \times 10^{20} \text{ cm}^{-3}$.

The glass-forming matrix system for activation by erbium ions was chosen on the basis of our previous studies, which showed that glasses of similar compositions have high transparency in the IR range, resistance to crystallization, and that high-quality optical elements and fibers can be successfully made from them [5–8]. The binary glass TeO₂-WO₃ was the basis, the matrix for the compositions used, and compares favorably with other widely studied compositions based on TeO₂-ZnO, with higher stability and solubility of REI, better mechanical properties, and significantly lower values of thermal expansion coefficient [20,31,32].

Lanthanum oxide La₂O₃ was included in the composition of tungsten–tellurite glass to increase the resistance to crystallization and for convenience of introducing erbium oxide. Bismuth oxide Bi₂O₃ was added to modify the refractive index of the core when creating light-guide structures.

The glasses were prepared from high-purity tellurium dioxide (TeO₂) obtained by vacuum distillation and from commercially available high-purity tungsten (WO₃), bismuth (Bi₂O₃), lanthanum (La₂O₃), and erbium (Er₂O₃) oxides. The total content of the 3d-transition metal impurities, most actively absorbed in the IR region, in the initial oxide mixture did not exceed 2 ppm wt [6].

The sample preparation technique included a number of successive stages: reduced pressure drying of the initial oxides batch, melting at 800 °C for several hours, lowering the temperature of the glass-forming melt and casting samples into a cylindrical mold of silica glass, annealing at the glass transition temperature, and slow cooling to room temperature. After cooling to room temperature, the castings were mechanically cut, ground, and polished for further study. Tablets 0.2 cm thick were used for the majority of optical measurements, while longer samples (0.6–1.5 cm long) were applied for OH volume absorption evaluation of erbium containing compositions (Figure 1). The prepared samples were optically homogeneous and did not contain large scattering defects in the volume; the samples with the highest concentration of Er₂O₃ (2 and 4 mol%) were characterized by a darker color.

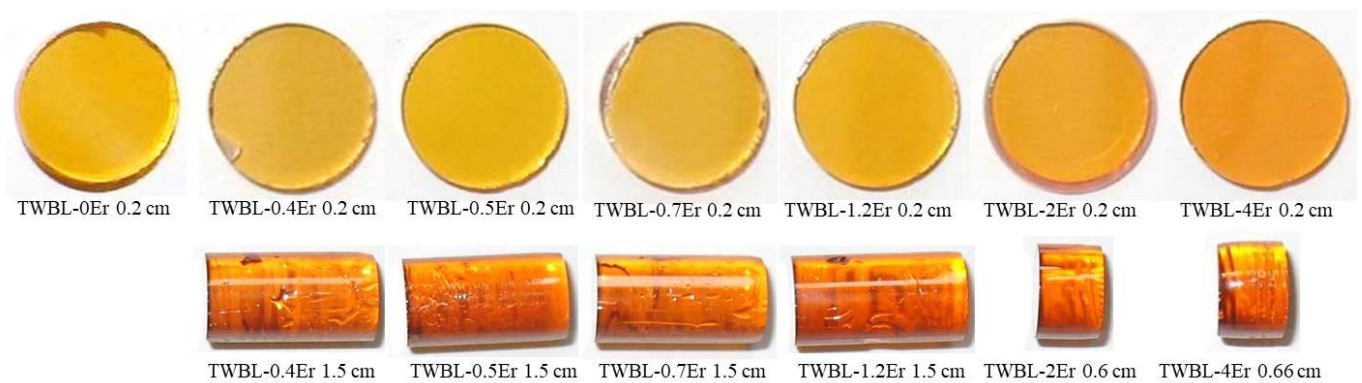


Figure 1. Photographs of the polished discs (tablets) and cylinders made of $\text{TeO}_2\text{-WO}_3\text{-Bi}_2\text{O}_3\text{-(4-x)La}_2\text{O}_3\text{-xEr}_2\text{O}_3$ glasses.

2.2. Methods

Differential scanning calorimetry (DSC) data were obtained on a Netzsch DSC 404 F1 Pegasus device. Samples of glass in the form of disks with a diameter of ~ 5 mm and a thickness of ~ 1 mm were used. Measurements were carried out in platinum crucibles in the temperature range of 300–950 K, at a thermal scanning rate of 10 K/min in a stream of pure argon, with a flow rate of 80 mL/min.

The transmittance spectra of the series TWBL-xEr were recorded with Lambda 900 spectrometer in the visible and near-IR regions and by a IR Nicolet 6700 Fourier spectrometer in the IR range. Absorption spectra inside the hydroxyl groups absorption band were calculated from the IR transmittance spectra by the expression $\ln(100/T\%)$, taking into account Fresnel reflection by subtracting the straight line. The volume absorption coefficient of hydroxyl groups in the band maximum was calculated using the formula $\alpha = (\ln(100/T\%) - 2\beta)/L$ (cm^{-1}); where L (cm) is the sample length, and 2β is the absorption by surface hydroxyl groups at the ends.

The refractive indices were measured using a prism-coupler Metricon-2010 at the wavelengths 633, 969, and 1539 nm. Three scans were made during each measurement; the error was estimated to be ± 0.0005 .

The luminescence spectra were recorded with a photovoltaic InSb detector P5968, using the excitation under pumping laser diode 975 nm with a power of 0.5 W. The radiation was focused on the sample using a lens; the scattered emission radiation was collected using another lens at the input slit of the monochromator MDR-2. A filter was used to cut off the pump spectrum. The kinetics of the luminescence were registered according to the same scheme, using a LeCroy oscilloscope and 976 nm optical parametric oscillator excitation with a pulse duration of ~ 5 ns. The decay curves for the ${}^4\text{I}_{13/2}\text{-}{}^4\text{I}_{15/2}$ transition were obtained directly from 1.53 emission data, and the lifetimes of the ${}^4\text{I}_{11/2}$ level were determined by recording the 0.98 μm emission using an infrared PMT with a photocathode having a time response of ~ 20 ns.

3. Results

3.1. Thermal Properties

The thermograms of the differential scanning calorimetry of the TWBL-xEr series are shown in Figure 2. The insert shows the DSC curves imposed in the temperature area of the glass transition, to illustrate the absence of the dependence of the glass transition temperature on the concentration of erbium oxide.

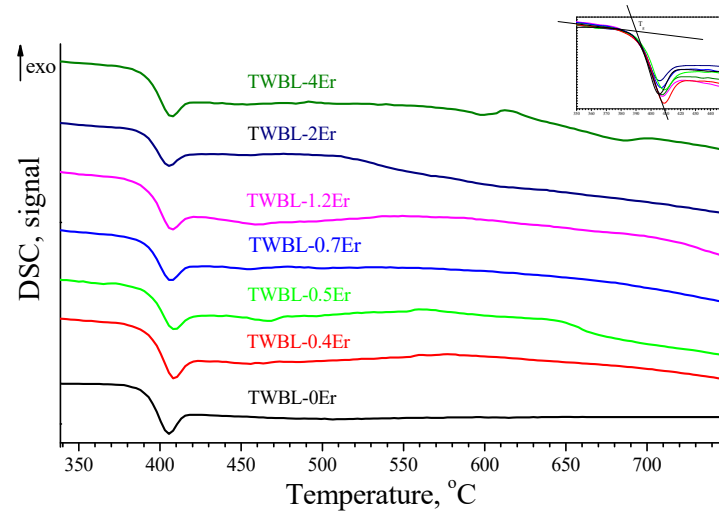


Figure 2. DSC-thermograms of $\text{TeO}_2\text{-WO}_3\text{-Bi}_2\text{O}_3\text{-(4-x)La}_2\text{O}_3\text{-xEr}_2\text{O}_3$ glasses, $x = 0; 0.4; 0.5; 0.7; 1.2; 2; 4$ mol% (heating rate 10 K/min).

There are no clear thermal effects of the crystallization and melting of crystals in the thermograms, which indicates the crystallization stability of the glasses of the series. Increasing the concentration of erbium oxide to 4 mol% practically does not change the glass transition temperature, which is equal to ~ 390 °C for all samples (insert in Figure 2). Thus, replacing lanthanum oxide with an equimolar amount of erbium oxide allows activating the core with Er ions, without changing the viscosity properties. This is very important in the process of making fibers.

3.2. Transmission Spectra and Hydroxyl Groups Absorption

The TWBL-xEr glasses have high transparency in the visible and IR regions, from 0.47 to 5.3 μm . The spectra of the samples in the visible and IR regions are shown in Figures 3 and 4. The absence of characteristic absorption bands of 3d-transition metals and undesirable impurity RE elements throughout the transparency area confirms the low impurity content.

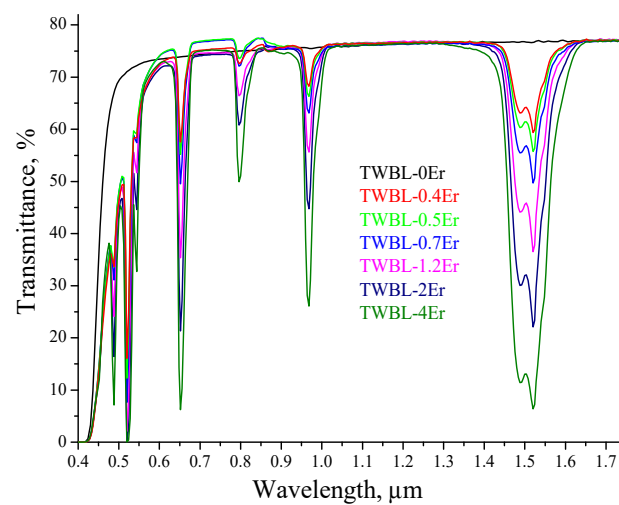


Figure 3. Visible and near-IR transmission spectra of $\text{TeO}_2\text{-WO}_3\text{-Bi}_2\text{O}_3\text{-(4-x)La}_2\text{O}_3\text{-xEr}_2\text{O}_3$ glass samples 0.2 cm thick, $x = 0; 0.4; 0.5; 0.7; 1.2; 2; 4$ mol%.

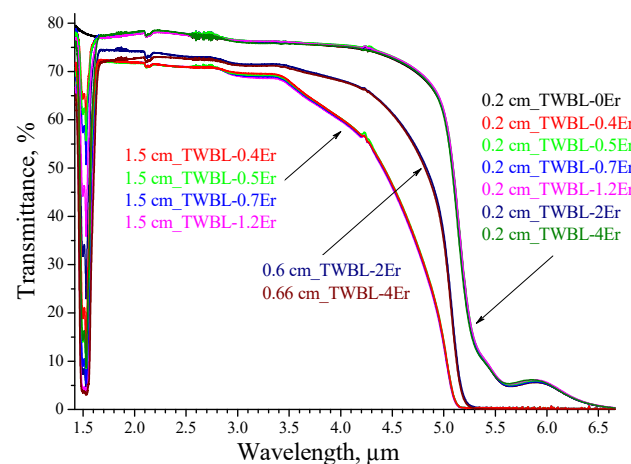


Figure 4. IR transmission spectra of $\text{TeO}_2\text{-WO}_3\text{-Bi}_2\text{O}_3\text{-(4-x)La}_2\text{O}_3\text{-xEr}_2\text{O}_3$ glass samples with different thicknesses.

The transmission spectra in the short-wave region contain typical Er^{3+} absorption bands, with peaks at 1530, 798, 653, 543, 521, and 489 nm corresponding to the absorption from the ground state of $^4\text{I}_{15/2}$ to the excited levels of $^4\text{I}_{13/2}$, $^4\text{I}_{9/2}$, $^4\text{F}_{9/2}$, $^4\text{S}_{3/2}$, $^2\text{H}_{11/2}$, and $^4\text{F}_{7/2}$. The intensity of the absorption peaks of erbium increases with its concentration. For pumping, while studying the luminescent characteristics of glasses and fibers, an absorption band corresponding to the $^4\text{I}_{15/2}\text{-}^4\text{I}_{11/2}$ transition, with a maximum at about 0.98 μm , was chosen. The absorption coefficient in this band is directly proportional to the concentration of Er_2O_3 (Figure 3).

The thin discs of TWBL-xEr glass, with a thickness of 2 mm (tablets, Figure 1), have a high transmittance at a level of at least 20% in the near and mid-IR ranges, up to a wavelength of ~ 5.3 μm (Figure 4). It is possible to note absorption bands at 5.4 and 5.7 μm in the spectra of the tablets, characteristic of the overtones of O=W bond vibrations in single and paired O= WO_5 centers in the first case, and of a combination of O=W and W-O-W vibrations in pairs of single O= WO_5 centers in the second [6]. The absorption bands of hydroxyl groups, with peaks of about 2.3, 3, and 4.4 microns characteristic of tellurite glasses obtained by the traditional method in open systems, are indistinguishable in the spectra of TWBL-xEr tablets. To calculate the volume absorption coefficient of the hydroxyl groups, samples of glasses in the form of longer cylinders (0.6–1.5 cm long) were used (Figure 1). In the transmission spectra of such samples, an absorption band with a maximum near 3 microns appears and can be mathematically processed (Figure 4).

The absorption spectra inside the hydroxyl groups absorption band, calculated from IR transmittance spectra by the expression $\ln(100/T\%)$, are plotted in Figure 5.

The absorption values of hydroxyl in samples of the TWBL-xEr series at the maximum of the band were found to be 0.007 for TWBL-0.4Er; 0.01 for TWBL-0.5Er; 0.011 for TWBL-0.7Er; 0.012 for TWBL-1.2Er; 0.01 for TWBL-2Er; and 0.009 for TWBL-4Er. The volume absorption coefficient of hydroxyl groups in the band maximum can be calculated from: α (cm^{-1}) = $(\ln(100/T\%) - 2\beta)/L$; where L (cm) is the sample length, β is the absorption at the two ends by hydroxyl groups adsorbed from the air or during polishing [5,32,33]. Taking into account the surface absorption of hydroxyl groups (on average $2\beta \approx 0.003$ for polished samples of tungsten-tellurite glasses [32,33]) and the actual length of the samples, the volume absorption coefficients at the band peak of ~ 3 μm were calculated (Table 1). The values are in the range of 0.003–0.011 cm^{-1} , which corresponds to the concentration of hydroxyl groups at the level of $n \times 10^{16}$ cm^{-3} [5,33,34]. Thus, the concentration of hydroxyl groups is inferior to the concentration of Er^{3+} by at least 10^4 times, allowing excluding the influence of this important impurity on the accuracy of determining the emission characteristics. A very important conclusion from a practical point of view is that

there is no deterioration in the effectiveness of our method for removing hydroxyl groups with an increase in the concentration of erbium in the glass-forming melt.

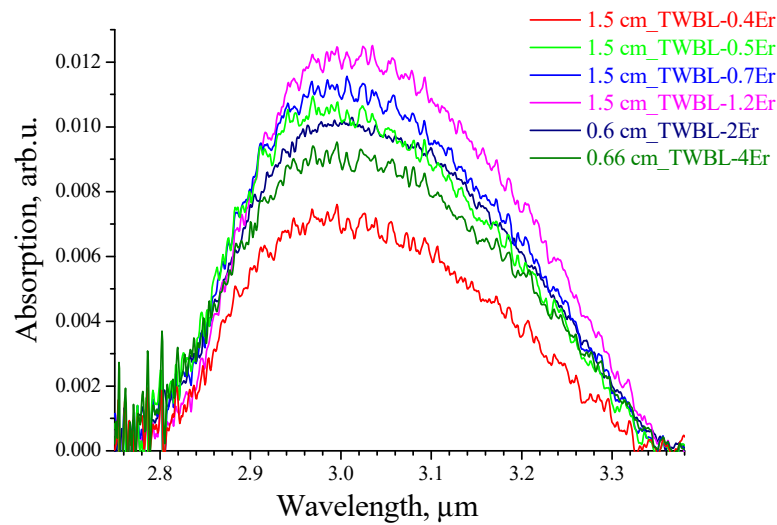


Figure 5. Absorption spectra of $\text{TeO}_2\text{-WO}_3\text{-Bi}_2\text{O}_3\text{-(4-x)La}_2\text{O}_3\text{-xEr}_2\text{O}_3$ glass samples with different thicknesses within the hydroxyl groups band.

3.3. Refraction Index

The values of the linear refractive index were determined for samples with Er_2O_3 contents of 0; 1.2; 4 mol% (TWBL-0Er, TWBL-1.2Er, TWBL-4Er). The dependence of the refractive index values on the concentration of erbium oxide at wavelengths of 633, 969, and 1539 nm is shown in Figure 6. The introduction of erbium oxide into the tungsten–tellurite matrix by replacing lanthanum oxide leads to a very slight decrease in the refractive index, even at high dopant concentrations; the values of the slope of the lines are in the order of -0.001 (Figure 6). Having only a minor change in the refractive index is highly desirable when designing fibers with a core activated with Er^{3+} .

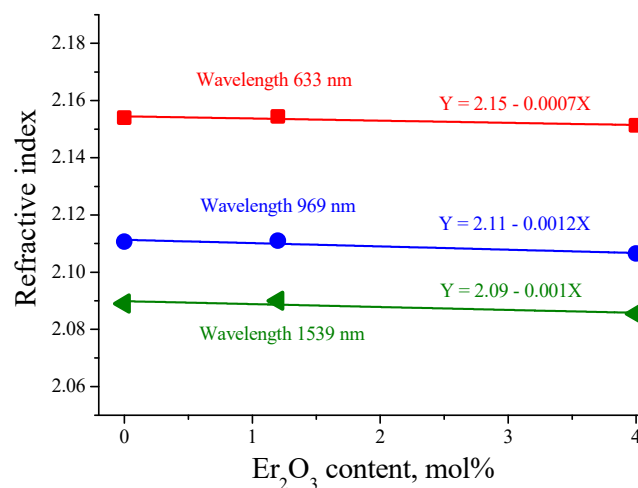


Figure 6. Refractive index of $\text{TeO}_2\text{-WO}_3\text{-Bi}_2\text{O}_3\text{-(4-x)La}_2\text{O}_3\text{-xEr}_2\text{O}_3$ glass samples versus Er_2O_3 concentration for wavelengths of 633, 969, and 1539 nm.

3.4. Luminescent Properties

At the excitation at $0.975 \mu\text{m}$, broad luminescence bands with maxima at ~ 1.53 and $\sim 2.75 \mu\text{m}$, corresponding to electronic transitions ${}^4\text{I}_{13/2}\text{-}{}^4\text{I}_{15/2}$ and ${}^4\text{I}_{11/2}\text{-}{}^4\text{I}_{13/2}$ of Er^{3+} for TWBL-xEr series glasses, were observed.

Figure 6 presents the experimental normalized luminescence spectra inside the Er^{3+} band with a peak at $1.53 \mu\text{m}$ of the $\text{TeO}_2\text{-WO}_3\text{-Bi}_2\text{O}_3\text{-(4-x)La}_2\text{O}_3\text{-xEr}_2\text{O}_3$ glasses with different Er_2O_3 contents. The emission bandwidth and the luminescence intensity near $1.53 \mu\text{m}$ increase with increasing Er^{3+} concentration; the samples with an erbium oxide content of 1.2 and 2% have the highest values; and an increase in concentration leads to a decrease in these characteristics of emission (Figures 7 and 8).

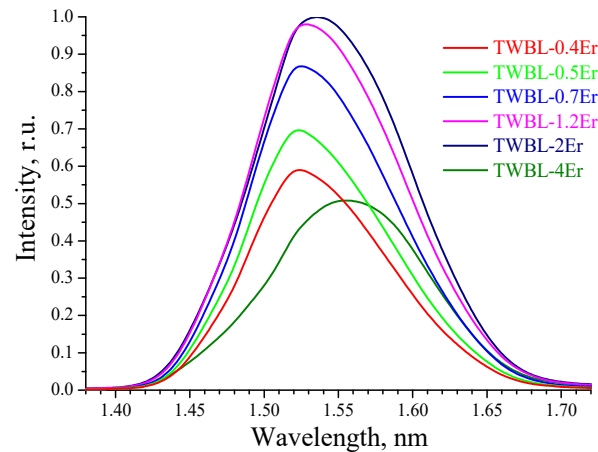


Figure 7. Luminescence band of Er^{3+} with peak at $1.53 \mu\text{m}$ of the $\text{TeO}_2\text{-WO}_3\text{-Bi}_2\text{O}_3\text{-(4-x)La}_2\text{O}_3\text{-xEr}_2\text{O}_3$ glasses with different Er_2O_3 contents.

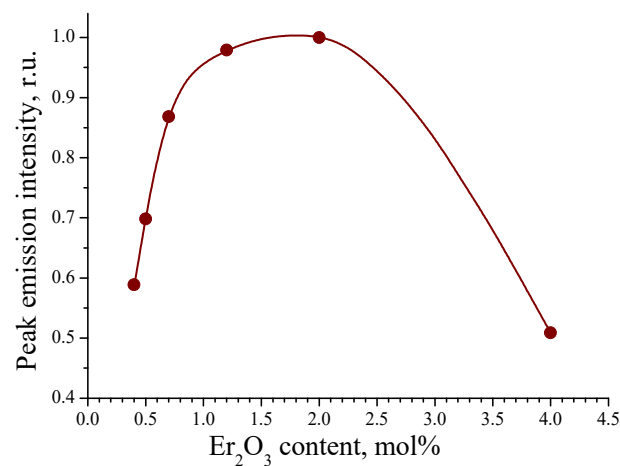


Figure 8. The $1.53 \mu\text{m}$ luminescence peak intensity as a function of Er_2O_3 content.

In the region of low erbium oxide concentrations (up to 0.7 mol%), the intensity increases strongly; in the region of medium concentrations (1.2–2 mol%), the intensity increases insignificantly; and with a further increase in the concentration, the $1.53 \mu\text{m}$ emission intensity drops.

This may be mainly due to the complete absorption of the pump radiation at the initial stage. However, when the Er^{3+} concentration becomes close enough to the absorption saturation, the increase in the radiation intensity slows down. At the same time, the distance between Er^{3+} ions becomes closer, and the upconversion effect of Er^{3+} grows with an increase in its concentration. This reduces the population of the $^4\text{I}_{13/2}$ level and leads to a sharp decrease in the emission intensity.

The behavior of the emission bandwidth as the concentration increases to 1.2 mol% can be explained by an increase in the variety of dopant sites in the glass matrix occupied by Er^{3+} ions, together with an increase in the number of ions. The luminescence spectrum broadens at this stage. Further termination of the broadening of the spectrum, and its

narrowing at the highest erbium concentration, is associated with the occupation of all possible dopant places and with the increase of upconversion intensity. Similar effects were observed in [25].

The experimental normalized luminescence spectra and the luminescence peak intensity dependence on the Er_2O_3 content for the Er^{3+} band near $2.75 \mu\text{m}$ for TWBL-xEr series glasses are presented in Figures 9 and 10, respectively. The luminescence intensity and bandwidth increase non-linearly with an increase in the doping level; there is no saturation of the dependences (Figures 9 and 10). The highest emission bandwidth and luminescence intensity values were found for the sample with the highest dopant content. The observed behavior can be explained by the same effects as in the case of the $1.53 \mu\text{m}$ band, but in the absence of an up-conversion from this level. Thus, high concentrations of the dopant can be used when the transition ${}^4\text{I}_{11/2} \rightarrow {}^4\text{I}_{13/2}$ of Er^{3+} is exploited.

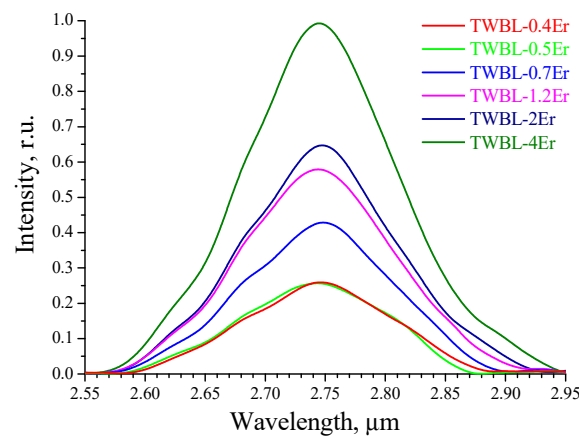


Figure 9. Luminescence band of Er^{3+} at $2.75 \mu\text{m}$ of the $\text{TeO}_2\text{-WO}_3\text{-Bi}_2\text{O}_3\text{-(4-x)La}_2\text{O}_3\text{-xEr}_2\text{O}_3$ glasses with different Er_2O_3 contents. Excitation 975 nm , 0.5 W .

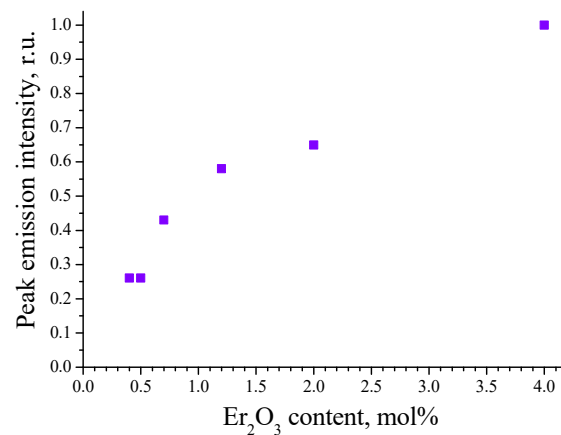


Figure 10. The $2.75 \mu\text{m}$ luminescence peak intensity versus Er_2O_3 content.

The lifetimes of the ${}^4\text{I}_{11/2}$ level of Er^{3+} were measured by registration of the $0.98 \mu\text{m}$ emission, the decay curves for glasses of the TWBL-xEr are plotted in Figure 11. The measured lifetimes of the ${}^4\text{I}_{11/2}$ level of Er^{3+} ion were 113 , 113 , and $104 \mu\text{s}$ for the Er_2O_3 contents of 0.4 , 1.2 , and $4 \text{ mol}\%$, respectively. The ${}^4\text{I}_{13/2}$ Er level lifetimes were measured by registering the $1.53 \mu\text{m}$ emission. The measured lifetimes of the ${}^4\text{I}_{13/2}$ level of Er^{3+} ion were 7.0 and 6.5 ms for the Er_2O_3 contents of 0.4 and $4 \text{ mol}\%$, respectively. An exponential attenuation of the luminescence intensity was observed when the excitation is removed, presumably the excited ions interact weakly with neighboring ions in the ground state.

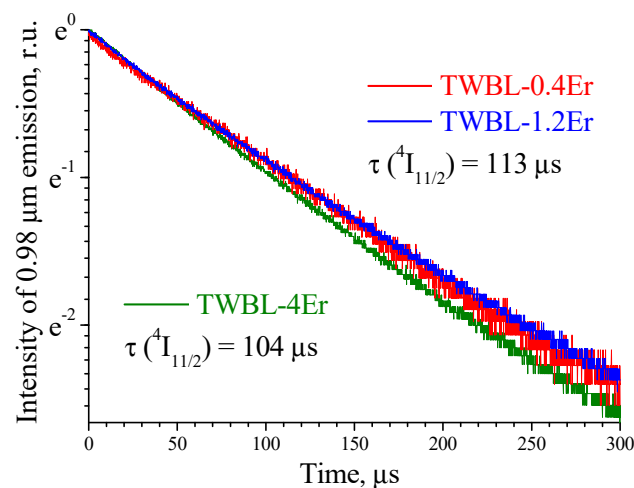


Figure 11. Decay curves of 0.98 μm luminescence from ${}^4\text{I}_{11/2}$ level for $\text{TeO}_2\text{-WO}_3\text{-Bi}_2\text{O}_3\text{-(4-x)La}_2\text{O}_3\text{-xEr}_2\text{O}_3$ glasses with Er_2O_3 contents of 0.4, 1.2, and 4 mol%.

For both ${}^4\text{I}_{11/2}$ and ${}^4\text{I}_{13/2}$ energy levels, a 10-fold increase in concentration led to a decrease in the lifetime by only 10%, due to non-radiative effects from concentration quenching. A slow reduction in the luminescence lifetimes, with a large increase in the Er^{3+} concentration, indicates weak concentration quenching. The possibility of creating high concentrations of dopant in the glass and weak concentration quenching confirms the absence of Er^{3+} ion clustering in the glasses [25].

4. Discussion

The properties of $\text{TeO}_2\text{-WO}_3\text{-Bi}_2\text{O}_3\text{-La}_2\text{O}_3\text{-Er}_2\text{O}_3$ glasses were studied depending on erbium oxide concentration. There were no clear thermal effects of the crystallization and melting of crystals on the DSC data; the glasses were resistant to crystallization up to 4 mol% Er_2O_3 . Increasing the concentration of erbium oxide to 4 mol% did not practically change the glass transition temperature, which was equal to $\sim 390^\circ\text{C}$ for all samples. Thus, replacing lanthanum oxide with an equimolar amount of erbium oxide allows activating the core with Er^{3+} , without changing the viscosity properties.

The introduction of erbium oxide by replacing lanthanum oxide leads to an insignificant change in the refractive index, even at high dopant concentrations. This is highly desirable when designing fibers with a core activated with Er^{3+} .

The considered glasses had high transmittance in the 4.7–5.3 μm range, the absorption bands of the hydroxyl groups at about 2.3, 3, and 4.4 μm , typical for ordinary tellurite glass samples, were indistinguishable for the thin specimens. The concentration of hydroxyl groups was inferior to the concentration of Er^{3+} by at least 10^4 times, allowing excluding the influence of this important impurity on the accuracy of determining the emission characteristics. There is no deterioration in the effectiveness of the method for hydroxyl group removal with an increase in the concentration of erbium in the glass-forming melt.

The Er_2O_3 -concentration dependencies for the luminescence characteristics were found for the ${}^4\text{I}_{13/2}\text{-}{}^4\text{I}_{15/2}$ and ${}^4\text{I}_{11/2}\text{-}{}^4\text{I}_{13/2}$ transitions of the Er^{3+} ion under 0.975 μm pumping. The dependence of the bandwidth and the luminescence intensity at the ${}^4\text{I}_{13/2}\text{-}{}^4\text{I}_{15/2}$ transition have a maximum, after which the emission characteristics are deteriorated; for the ${}^4\text{I}_{11/2}\text{-}{}^4\text{I}_{13/2}$ transition the bandwidth and intensity increase without the observed saturation. The measured lifetimes of the ${}^4\text{I}_{11/2}$ level of the Er^{3+} ion were 110 and 100 μs , and the ${}^4\text{I}_{13/2}$ levels of the Er^{3+} ion were 7.0 and 6.5 ms for the Er_2O_3 contents of 0.4 and 4 mol%, respectively; demonstrating a decrease with an increase in the activator concentration.

5. Conclusions

A series of TeO₂-WO₃-Bi₂O₃-La₂O₃-Er₂O₃ glasses was synthesized from high-purity oxides in a purified oxygen flow inside a sealed silica chamber. Binary TeO₂-WO₃ glass was the basis, La₂O₃ was included to increase the resistance to crystallization and for convenience of introducing an Er³⁺ activator, and Bi₂O₃ was added to evaluate the practice of modifying the refractive index of the core of the step-index fibers. High-quality optical elements and fibers had previously been successfully manufactured from similar glasses, and detailed studies of the doping features are necessary to improve the active devices.

The properties important for use in photonics and fiber optics were studied, depending on erbium concentration. To obtain the most accurate data, special attention was paid to reducing the concentration of impurities, primarily hydroxyl groups, through the use of pure starting materials and original synthesis technology. In all samples of the series, an extremely low content of hydroxyl groups $\sim n \times 10^{16} \text{ cm}^{-3}$ was achieved, in order to guarantee there were no effects on the luminescence properties of Er³⁺.

The transparency range of the considered glasses extended from 4.7 to 5.3 μm . The introduction of erbium oxide led to an insignificant changes in the refractive index, resistance to crystallization, and glass transition temperature. This is very important for production of optical fibers with a core activated with Er³⁺.

The studies of the emission characteristics show that low concentrations of the activator are preferable for using emission at the ⁴I_{13/2}-⁴I_{15/2} transition. To use the emission at the ⁴I_{11/2}-⁴I_{13/2} transition, it is preferable to achieve high concentrations of the activator.

The results obtained confirm the high applicability of these glasses for creating active fiber-optic devices and are useful for calculating specific laser fibers.

Author Contributions: Conceptualization, V.V.D. and V.V.K.; methodology, V.V.D. and A.D.P.; validation, V.V.D. and V.V.K.; formal analysis, V.V.D., V.V.K. and A.D.P.; investigation, V.V.D., S.E.M. and V.V.K.; resources, V.V.D., V.V.K. and A.V.K.; data curation, V.V.D. and S.E.M.; writing—original draft preparation, V.V.D. and V.V.K.; writing—review and editing, V.V.D. and A.V.K.; visualization, V.V.D. and V.V.K.; supervision, V.V.D. and A.V.K.; project administration, V.V.D. and A.V.K.; funding acquisition, V.V.D. and A.V.K. All authors have read and agreed to the published version of the manuscript.

Funding: The work was supported by the Center of Excellence «Center of Photonics» funded by the Ministry of Science and Higher Education of the Russian Federation, contract No. 075-15-2020-906.

Conflicts of Interest: The authors declare no conflict of interest.

References

- Jha, A.; Richards, B.; Jose, G.; Teddy-Fernandez, T.; Joshi, P.; Jiang, X.; Lousteau, J. Rare-earth ion doped TeO₂ and GeO₂ glasses as laser materials. *Prog. Mater. Sci.* **2012**, *57*, 1426–1491. [[CrossRef](#)]
- El-Mallawany, R.A.H. *Tellurite Glasses Handbook: Physical Properties and Data*; CRC Press: Boca Raton, FL, USA, 2016.
- Smayev, M.P.; Dorofeev, V.V.; Moiseev, A.N.; Okhrimchuk, A.G. Femtosecond laser writing of a depressed cladding single mode channel waveguide in high-purity tellurite glass. *J. Non-Cryst. Solids* **2018**, *480*, 100–106. [[CrossRef](#)]
- Yakovlev, A.I.; Snetkov, I.L.; Dorofeev, V.V.; Motorin, S.E. Magneto-optical properties of high-purity zinc-tellurite glasses. *J. Non-Cryst. Solids* **2018**, *480*, 90–94. [[CrossRef](#)]
- Anashkina, E.A.; Dorofeev, V.V.; Koltashev, V.V.; Kim, A.V. Development of Er³⁺-doped high-purity tellurite glass fibers for gain-switched laser operation at 2.7 μm . *Opt. Mater. Express* **2017**, *7*, 4337–4351. [[CrossRef](#)]
- Dorofeev, V.V.; Moiseev, A.N.; Churbanov, M.F.; Kotereva, T.V.; Chilyasov, A.V.; Kraev, I.A.; Pimenov, V.G.; Ketkova, L.A.; Dianov, E.M.; Plotnichenko, V.G.; et al. Production and properties of high purity TeO₂-WO₃-(La₂O₃, Bi₂O₃) and TeO₂-ZnO-Na₂O-Bi₂O₃ glasses. *J. Non-Cryst. Solids* **2011**, *357*, 2366–2370. [[CrossRef](#)]
- Anashkina, E.A.; Andrianov, A.V.; Dorofeev, V.V.; Kim, A.V. Toward a mid-infrared femtosecond laser system with suspended-core tungstate-tellurite glass fibers. *Appl. Opt.* **2016**, *55*, 4522–4530. [[CrossRef](#)] [[PubMed](#)]
- Muravyev, S.V.; Anashkina, E.A.; Andrianov, A.V.; Dorofeev, V.V.; Motorin, S.E.; Koptev, M.Y.; Kim, A.V. Dual-band Tm³⁺-doped tellurite fiber amplifier and laser at 1.9 μm and 2.3 μm . *Sci. Rep.* **2018**, *8*, 16164. [[CrossRef](#)] [[PubMed](#)]
- Denker, B.I.; Dorofeev, V.V.; Galagan, B.I.; Koltashev, V.V.; Motorin, S.E.; Plotnichenko, V.G.; Sverchkov, S.E. 2.3 μm laser action in Tm³⁺-doped tellurite glass fiber. *Laser Phys. Lett.* **2019**, *16*, 015101. [[CrossRef](#)]
- Ebrahim-Zadeh, M.; Sorokina, I.T. *Mid-Infrared Coherent Sources and Applications*; Springer: Dordrecht, The Netherlands, 2008. [[CrossRef](#)]

11. Wartewig, S.; Neubert, R.H.H. Pharmaceutical applications of mid-IR and Raman spectroscopy. *Adv. Drug Deliv. Rev.* **2005**, *57*, 1144–1170. [[CrossRef](#)]
12. Mukherjee, A.; Von der Porten, S.; Patel, C.K.N. Standoff detection of explosive substances at distances of up to 150 m. *Appl. Opt.* **2010**, *49*, 2072–2078. [[CrossRef](#)]
13. Seddon, A.B. Mid-Infrared (IR)—A hot topic: The potential for using mid-IR light for non-invasive early detection of skin cancer in vivo. *Phys. Status Solidi B* **2013**, *250*, 1020–1027. [[CrossRef](#)]
14. Moiseev, A.N.; Dorofeev, V.V.; Chilyasov, A.V.; Pimenov, V.G.; Kotereva, T.V.; Kraev, I.A.; Ketkova, L.A.; Kosolapov, A.F.; Plotnichenko, V.G.; Koltashev, V.V. Low loss, high-purity $(\text{TeO}_2)_{0.75}(\text{WO}_3)_{0.25}$ glass. *Inorg. Mater.* **2011**, *47*, 665–669. [[CrossRef](#)]
15. Feng, X.; Qi, C.; Lin, F.; Hu, H. Tungsten tellurite glass a new candidate medium for Yb^{3+} -doping. *J. Non-Cryst. Solids* **1999**, *256–257*, 372–377. [[CrossRef](#)]
16. Dorofeev, V.V.; Moiseev, A.N.; Churbanov, M.F.; Snopatin, G.E.; Chilyasov, A.V.; Kraev, I.A.; Lobanov, A.S.; Kotereva, T.V.; Ketkova, L.A.; Pushkin, A.A.; et al. High purity TeO_2 - WO_3 - $(\text{La}_2\text{O}_3, \text{Bi}_2\text{O}_3)$ glasses for fiber-optics. *Opt. Mater.* **2011**, *33*, 1911–1915. [[CrossRef](#)]
17. Champarnaud-Mesjard, J.-C.; Thomas, P.; Marchet, P.; Frit, B.; Chagraoui, A.; Tairi, A. Glass Formation Study in the Bi_2O_3 - TeO_2 - WO_3 System. *Ann. Chim. Sci. Mater.* **1998**, *23*, 289–292. [[CrossRef](#)]
18. Kaky, K.M.; Lakshminarayana, G.; Baki, S.O.; Kityk, I.V.; Taufiq-Yap, Y.H.; Mahdi, M.A. Structural, thermal and optical absorption features of heavy metal oxides doped tellurite rich glasses. *Results Phys.* **2017**, *7*, 166–174. [[CrossRef](#)]
19. Yousef, E.; Hotzel, M.; Rüssel, C. Effect of ZnO and Bi_2O_3 addition on linear and non-linear optical properties of tellurite glasses. *J. Non-Cryst. Solids* **2007**, *353*, 333–338. [[CrossRef](#)]
20. Balueva, K.V.; Kut'in, A.M.; Plekhovich, A.D.; Motorin, S.E.; Dorofeev, V.V. Thermophysical characterization of TeO_2 - WO_3 - Bi_2O_3 glasses for optical applications. *J. Non-Cryst. Solids* **2021**, *553*, 120465. [[CrossRef](#)]
21. Boetti, G.N.; Lousteau, J.; Chiasera, A.; Ferrari, M.; Mura, E. Thermal stability and spectroscopic properties of erbium-doped niobic-tungsten-tellurite glasses for laser and amplifier devices. *J. Lumin.* **2012**, *13*, 1265–1269. [[CrossRef](#)]
22. El-Mallawany, R.; Ahmed, I.A. Thermal properties of multicomponent tellurite glass. *J. Mater. Sci.* **2008**, *43*, 5131–5138. [[CrossRef](#)]
23. Ersundu, A.E.; Karaduman, G.; Çelikkilek, M.; Solak, N.; Aydın, S. Effect of rare-earth dopants on the thermal behavior of tungsten-tellurite glasses. *J. Alloys Compd.* **2010**, *508*, 266–272. [[CrossRef](#)]
24. Ma, Y.; Guo, Y.; Huang, F.; Hu, L.; Zhang, J. Spectroscopic properties in Er^{3+} doped zinc- and tungsten-modified tellurite glasses for 2.7 μm laser materials. *J. Lumin.* **2014**, *147*, 372–377. [[CrossRef](#)]
25. Gomes, L.; Oermann, M.; Ebendor-Heidepriem, H.; Ottaway, D.; Monroe, T.; Felipe Henriques Librantz, A.; Jackson, S.D. Energy level decay and excited state absorption processes in erbium-doped tellurite glass. *J. Appl. Phys.* **2011**, *110*, 083111. [[CrossRef](#)]
26. Anashkina, E.A. Laser Sources Based on Rare-Earth Ion Doped Tellurite Glass Fibers and Microspheres. *Fibers* **2020**, *8*, 30. [[CrossRef](#)]
27. Li, J.; Li, S.; Hu, H.; Gan, F. Emission properties of $\text{Yb}^{3+}/\text{Er}^{3+}$ doped TeO_2 - WO_3 - ZnO glasses for Broadband Optical Amplifiers. *J. Mater. Sci. Technol.* **2004**, *20*, 139–142.
28. Oermann, M.R.; Ebendor-Heidepriem, H.; Li, Y.; Foo, T.C.; Monroe, T.M. Index matching between passive and active tellurite glasses for use in microstructured fiber lasers: Erbium doped lanthanum-tellurite glass. *Opt. Express* **2009**, *17*, 15578–15584. [[CrossRef](#)]
29. Zhan, H.; Zhou, Z.; He, J. Intense 2.7 μm emission of Er^{3+} -doped water-free fluorotellurite glasses. *Opt. Lett.* **2012**, *37*, 3408–3410. [[CrossRef](#)] [[PubMed](#)]
30. Anashkina, E.A.; Dorofeev, V.V.; Skobelev, S.A.; Balakin, A.A.; Motorin, S.E.; Kosolapov, A.F.; Andrianov, A.V. Microstructured fibers based on tellurite glass for nonlinear conversion of Mid-IR ultrashort optical pulses. *Photonics* **2020**, *7*, 51. [[CrossRef](#)]
31. Kut'in, A.M.; Plekhovich, A.D.; Dorofeev, V.V.; Moiseev, A.N.; Churbanov, M.F.; Markin, A.V. Thermophysical Properties of TeO_2 - WO_3 - La_2O_3 Glass. *J. Non-Cryst. Solids* **2013**, *377*, 16–20. [[CrossRef](#)]
32. Kut'in, A.M.; Plekhovich, A.D.; Balueva, K.V.; Motorin, S.E.; Dorofeev, V.V. Thermal properties of high purity zinc-tellurite glasses for fiber-optics. *Thermochim. Acta* **2019**, *673*, 192–197. [[CrossRef](#)]
33. Churbanov, M.F.; Moiseev, A.N.; Chilyasov, A.V.; Dorofeev, V.V.; Kraev, I.A.; Lipatova, M.M.; Kotereva, T.V.; Dianov, E.M.; Plotnichenko, V.G.; Kryukova, E.B. Production of high-purity TeO_2 - ZnO and TeO_2 - WO_3 glasses with the reduced content of OH-groups. *J. Optoelectron. Adv. Mater.* **2007**, *9*, 3229–3234.
34. Tatarintsev, B.V.; Yakhkind, A.K. The water content in tellurite glasses and its effect on infrared transmission. *Opt. Promyshlennost* **1975**, *3*, 40–43.